GROWTH AND CHARACTERIZATION OF MATERIALS FOR TUNABLE LASERS IN THE NEAR INFRARED SPECTRAL REGION

Principal Investigators
Richard C. Powell and Joel J. Martin

Department of Physics
Oklahoma State University
Stillwater, OK 74078-0444

NASA Research Grant NAG-1-694

Semi-annual Progress Report
1 August 1987 - 31 January 1988

INTRODUCTION

The work on this project during the report period can be divided into two thrust areas according to materials: $LiY_{1-x}Yb_xF_4$:RE and $LiNbO_3$:Mg,Cr,RE. The following two sections summarizes the crystal growth and spectroscopy work performed on these materials. Crystals grown under the sponsorship of this contract were sent to NASA Langley Research Center as they were produced.

The key personnel involved in the project during this time period were:

Crystal Growth	Spectroscopy
Prof. J.J. Martin, P.I.	Prof. R.C. Powell, P.I.
C. Hunt, technician	M.L. Kliewer, G.R.A.
A. Doddson, G.R.A.	

The major travel expense was for one of the principal investigators to attend the Tunable Solid State Laser Conference.

GROWTH OF $LiY_{(1-X)}Yb_XF_4$

Lithium yttrium fluoride, $LiYF_4$, has been used as a host material where a 3+ valence laser active dopant is desired. For a near infrared laser an alloy crystal of lithium yttrium-ytterbium fluoride doped with holmium may be interesting. $LiYF_4$ has the tetragonal scheelite crystal structure and we expect that the alloy crystals, for the lower Yb concentrations, should have the same structure. Figure 1 shows the phase diagram for the $LiF-YF_4$ system [1].

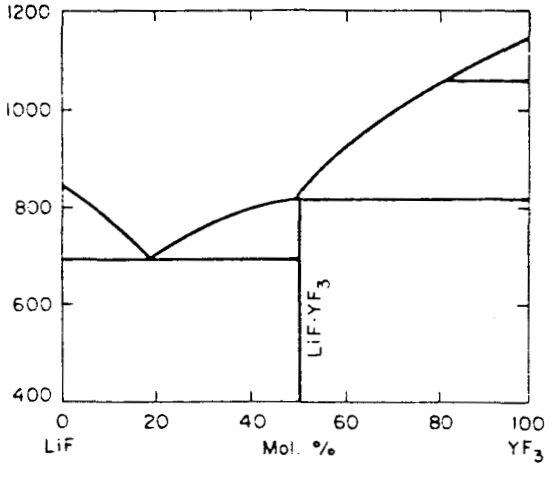

Figure 1. The phase diagram for the $LiF-YF_4$ system [1].

As shown in the diagram, the compound $LiYF_4$ is incongruently melting and transforms to liquid plus YF_3 at 819°C. Phase diagrams for the alloy system with ytterbium have not been determined; however, the phase diagrams for other rare-earths in $LiYF_4$ appear to be similar to the one in Fig. 1. While such phase diagrams suggest that the growth of single crystals may be difficult, $LiYF_4$ has been routinely grown by both the Bridgman and Czochralski methods [2,3].

Our initial attempts at growing $LiYF_4$ were made using the

same techniques that we have successfully used to grow a number of the fluoride perovskite componds such as $KMgF_3$. We started with a stoichiometric mixture of LiF and YF_3 in a vitreous carbon crucible. The starting materials were Johnson-Mathey Aesar optical grade LiF crystal cuttings and Johnson-Mathey REacton YF_3 powder. The crucible was then placed in our Bridgman furnace, the furnace tube was evacuated and heated to about 300°C overnight. After filling the system with argon, the temperature was raised to just above the 819°C melting point. The furnace was then rapidly cycled through its motion so that the material was frozen from the bottom. Then it was remelted and the furnace slowly raised so as to slowly cool the crucible from the bottom. After removal from the furnace, we found that about 60% of the material had been "blown out" of the crucible and that the remainder was a sintered powder. Fluorides such as YF_3 are often prepared from the carbonates and we suspect that residual carbonates, oxides, hyroxides, and adsorbed water are probably present in most commercially available powders. Our previous experience with the fluoride perovskites has been that the best crystals were grown when "crystal pieces" of, for example, KF and MgF_2 were used and that the lowest quality occured when one or more of the constituents were powders.

There are a number of reports describing the purification of $LiYF_4$ before and during crystal growth [3,4,5] by flowing HF gas over the material. The fluorine from the HF replaces the replaces the remaining carbonates or oxides and cleans up the hydroxides. Since an HF atmoshpere is not compatible with any of our existing crystal growth furnaces we set up a system for

treating the starting materials prior to the crystal growth runs. Figure 2 shows a schematic diagram of our system.

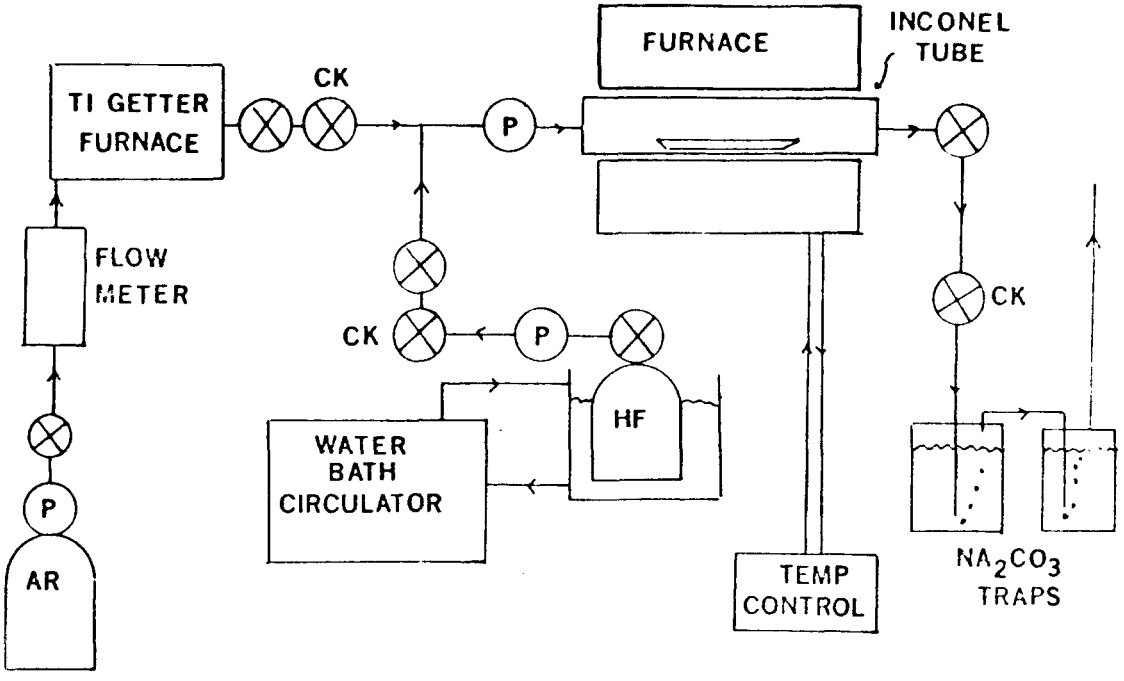

Figure 2. The HF pretreatment system.

Stoichiometeric mixtures of the consituents of the desired compound are placed in a vitreous carbon boat. The boat is then placed along with a grafoil cover in the Inconel furnace tube. After sealing the furnace tube, a gettered argon flow of 25ml/min is established. The programmed controller raises the furnace temperature up to the desired temperature; this is usually about 900°C for $LiYF_4$. We start the flow of HF when the furnace temperature reaches 750°C. The HF pressure is regulated by controlling the temperature of the water bath surrounding the HF cylinder. HF has a normal boiling point of 20°C. The furnace is held at temperature for one to two hours then programmed back to room temperature. The HF flow is maintained until the system has

cooled below 800°C; argon flow is continued throughout the entire process. About 24 hours are needed to go through the entire cycle. Normally, we load the system the night before a run, the programmable controller then runs it up part way over night. The resulting material is a clear polycrystalling lump.

The polycrystalline lump can then be used as starting material for either Bridgman or Czochralski crystal growth. So far, we have only carried out Bridgman growth. The first crystal growth runs were made with HF treated $LiYF_4$. These runs yielded very clear, single crystals with essentially no material loss during the run. After this success, a batch of $LiY_{0.99}Yb_{0.01}F_4$ was prepared by the HF pretreatment process. The first Bridgman run which was carried out at the same temperature as the $LiYF_4$ runs gave a sintered boule. A second run was then carried out with the temperature of the Bridgman furnace raised 30°C. This higher temperature run produced a very clear, single crystal of the 1% alloy compound. Evidently the melting point increases with increasing Yb content. The clarity of these crystals is much better than we normally obtain for the fluoride perovskites. They show essentially no scattering of a HeNe laser beam to the naked eye whereas $KMgF_3$ always shows some visible scattering.

We have demonstrated that the $LiY_{(1-x)}Yb_xF_4$ alloy crystal are growable. The next step is to prepare a batch of crystals of varying Yb content for optical tests. Once they have been prepared we will start making doped crystals. We also need to determine the actual Yb content of the crystals.

REFERENCES

1. R. E. Thoma, C. F. Weaver, H. A. Friedman, H. Insley, L. A. Harris, and H. L. Yakel, J. Phys. Chem., *65*, 1096 (1961).

2. R. Uhrin, R. F. Belt, and V. Rosati, J. Crystal Growth., *38*, 38 (1977).

3. D. A. Jones, B. Cockayne, R. A. Clay, and P. A. Forrester, J. Crystal Growth, *30*, 21 (1975).

4. B. Cockayne, J. G. Plant and R. A. Clay, J. Crystal Growth, *54*, 407 (1981).

5. R. C. Pastor, M. Robinson and W. M. Akutagawa, Mat. Res. Bull. *10*, 501 (1975).

$LiNbO_3$:Mg,Cr,RE CRYSTALS

The set of 8 crystals listed in Table I were grown in order to investigate the use of lithium niobate as a laser host material. The Mg is included in the crystals to reduce optical damage effects. The Cr ions provide broad absorption bands for pumping and a broad emission band for energy transfer to rare earth ions. The rare earth ions provide the sharp emission transitions for laser action.

TABLE I. $LiNbO_3$:Mg,Cr,RE Crystals

Material	Dopant Concentration	Sample I.D.
1. $LiNbO_3$:Mg,Cr	4.5% MgO 0.05 % Cr_2O_3	042087
2. $LiNbO_3$:Mg,Cr,Nd	4.5% MgO 0.05% Cr_2O_3 0.025% Nd_2O_3	090987
3. $LiNbO_3$:Mg,Cr,Tm	4.5% MgO 0.05% Cr_2O_3 0.025% Tm_2O_3	091687
4. $LiNbO_3$:Mg,Cr,Er	4.5% MgO 0.025% Cr_2O_3 0.1% Er_2O_3	093087
5. $LiNbO_3$:Mg,Cr,Ho	4.5% MgO 0.025% Cr_2O_3 0.1% Ho_2O_3	100687
6. $LiNbO_3$:Mg,Cr,Yb	4.5% MgO 0.025% Cr_2O_3 0.1% Yb_2O_3	102687
7. $LiNbO_3$:Mg,Cr,Tm	4.5% MgO 0.025% Cr_2O_3 0.1% Tm_2O_3	011588
8. $LiNbO_3$:Mg,Cr,Nd	4.5% MgO 0.025% Cr_2O_3 0.1% Nd_2O_3	011188

Figure 3 shows the absorption spectrum of Cr^{3+} in $LiNbO_3$:Mg (solid line) and the emission spectra (broken line) along with the positions of several of the rare earth energy levels in resonance with the emission band. Preliminary spectroscopy measurements have been made on these samples and complete, detailed investigations will be carried out during the next [illegible]

In addition to the standard spectroscopy measurements, the $LiNbO_3$:Mg,Cr sample was placed in a cavity and was pumped with the second harmonic (532 nm) of a Nd:YAG laser. Both end pumping and side pumping were attempted with fluences of up to 2.5 J/cm^2 at both room and low (12 K) temperatures. Surface damage occurred for fluences > 650 mJ/cm^2, half of what is needed for obtaining stimulated emission. The inability to obtain lasing of the material may be due losses associated with not having AR coating on the surfaces of the sample.

Figures 4 through 8 show the absorption spectra of the various RE ions in $LiNbO_3$:Mg,Cr crystals. The broad bands are associated with the Cr^{3+} absorption transitions while the sharp structure is due to rare earth absorption transitions. So far the fluorescence spectra have only been obtained on the Er^{3+} and Yb^{3+} doped crystals and the results are shown in Figs. 9 and 10. These spectra were obtained by pumping into the $^4T_2$ band of the Cr^{3+} ions. The emission of the $LiNbO_3$:Mg,Cr,Er sample is mainly associated with the broad band Cr^{3+} transition with some structure due to radiative reabsorption by the Er^{3+} ions. This indicates that Cr-Er radiationless energy transfer is weak. On the other hand, Yb emission is observed along with the Cr

emission in the $LiNbO_3$:Mg,Cr,Yb sample indicating strong Cr-Yb radiationless energy transfer.

In order to further investigate the energy transfer in $LiNbO_3$:Mg,Cr,Yb, the fluorescence lifetime of the Cr^{3+} emission was measured as a function of temperature and the results compared to those obtained on the $LiNbO_3$:Mg,Cr sample. These are shown in Fig. 11. Since the fluorescence emission in both of these samples is multi-exponential, the 1/e value of the decay is plotted. The energy transfer rate calculated from the difference in these decay rates is plotted versus temperature in Fig. 12. The results indicate that there is phonon assisted energy transfer taking place. This will be investigated further during the next report period.

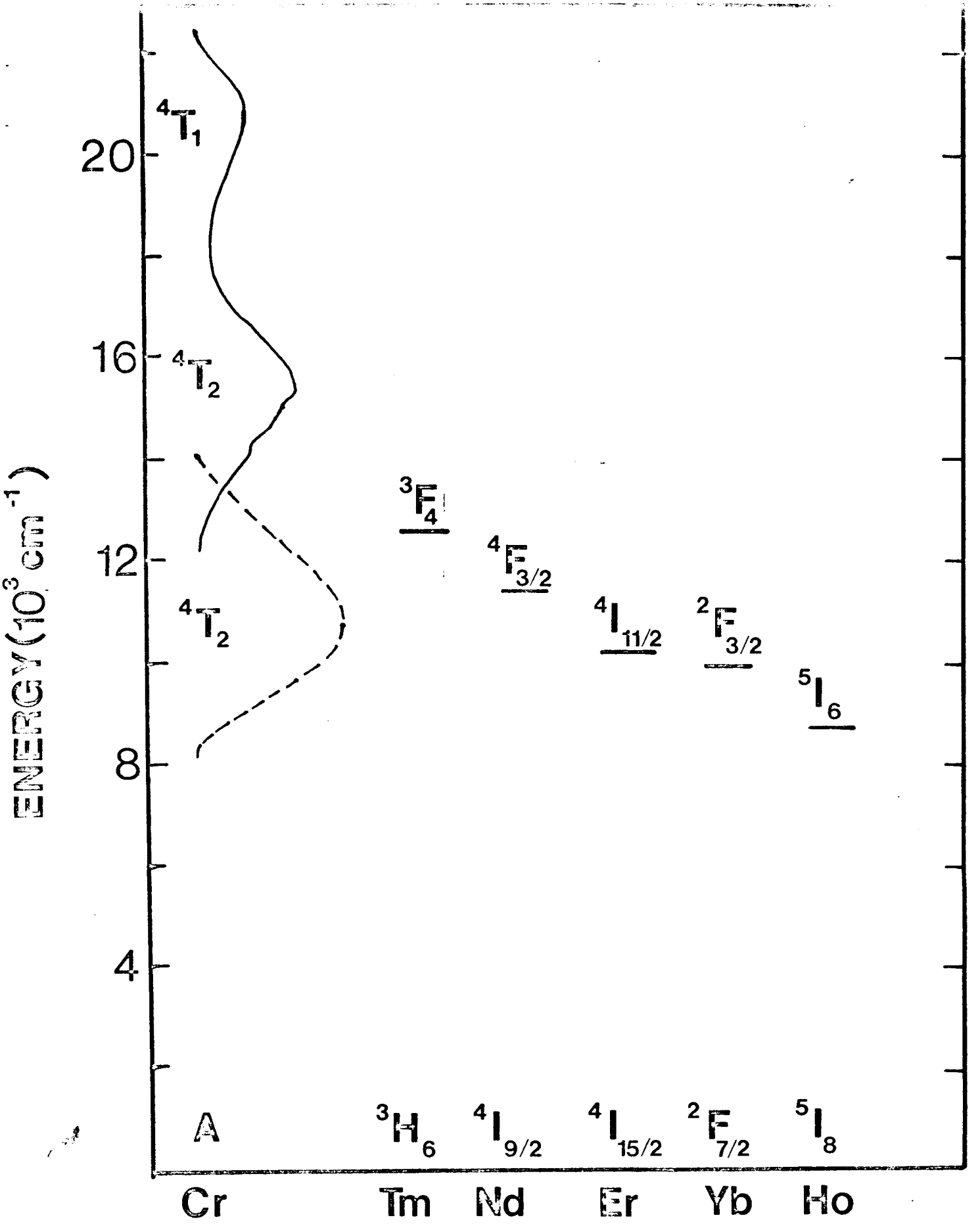

Figure 3. Spectra of Cr^{3+} in $LiNbO_3$:Mg and resonant RE energy levels.

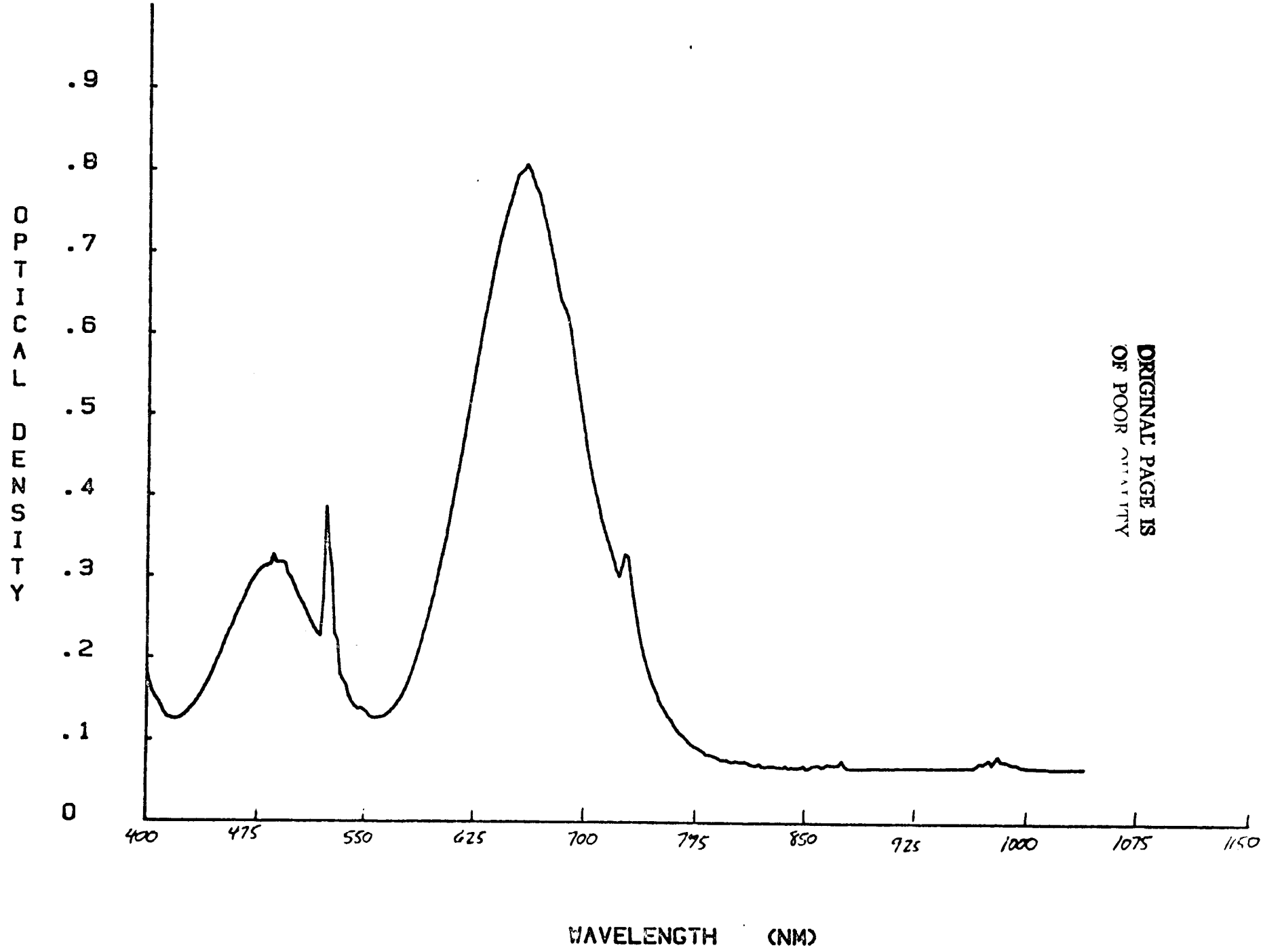

Figure 4. Absorption Spectrum of Er in $LiNbO_3$:Mg, Cr.

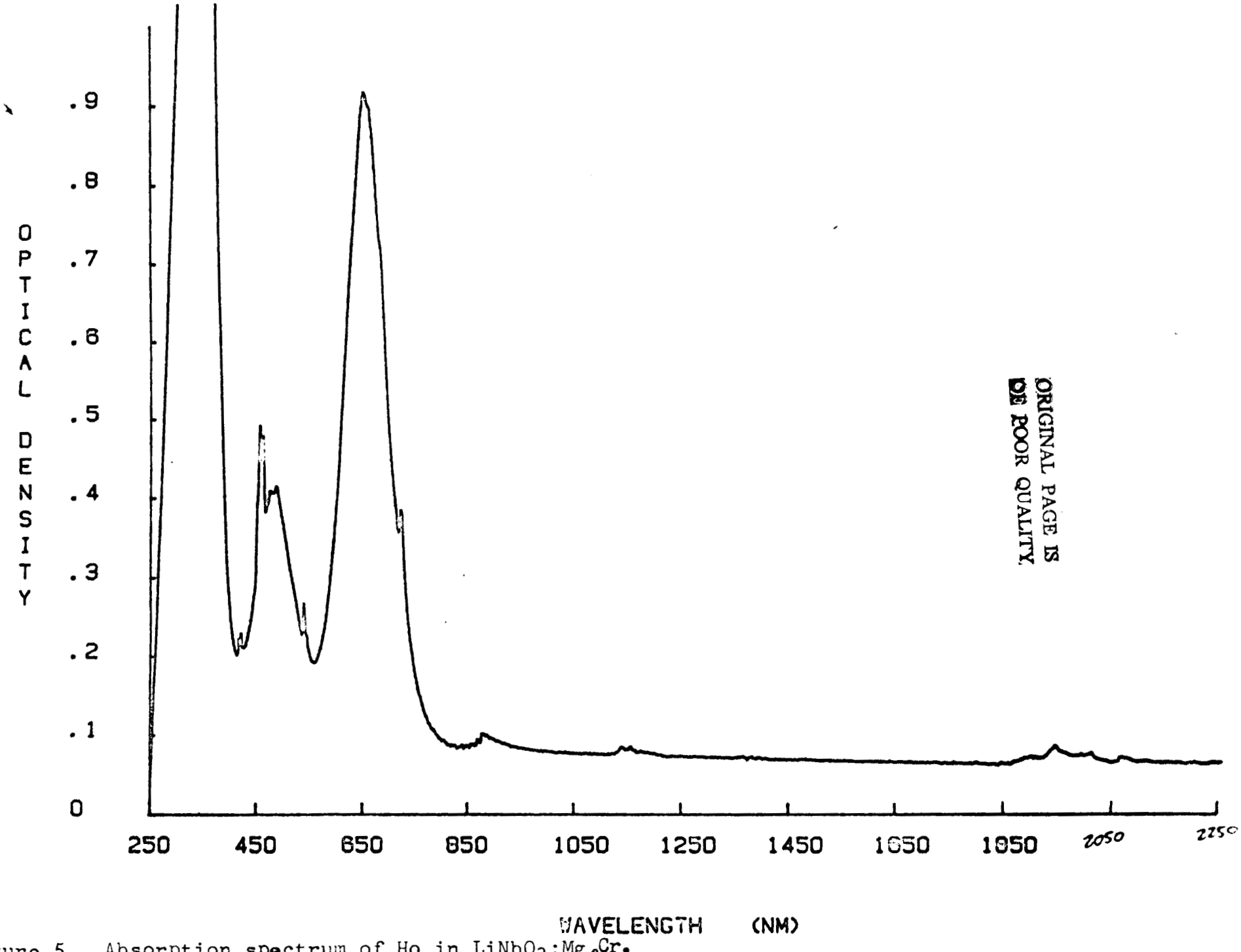

Figure 5. Absorption spectrum of Ho in $LiNbO_3$:Mg,Cr.

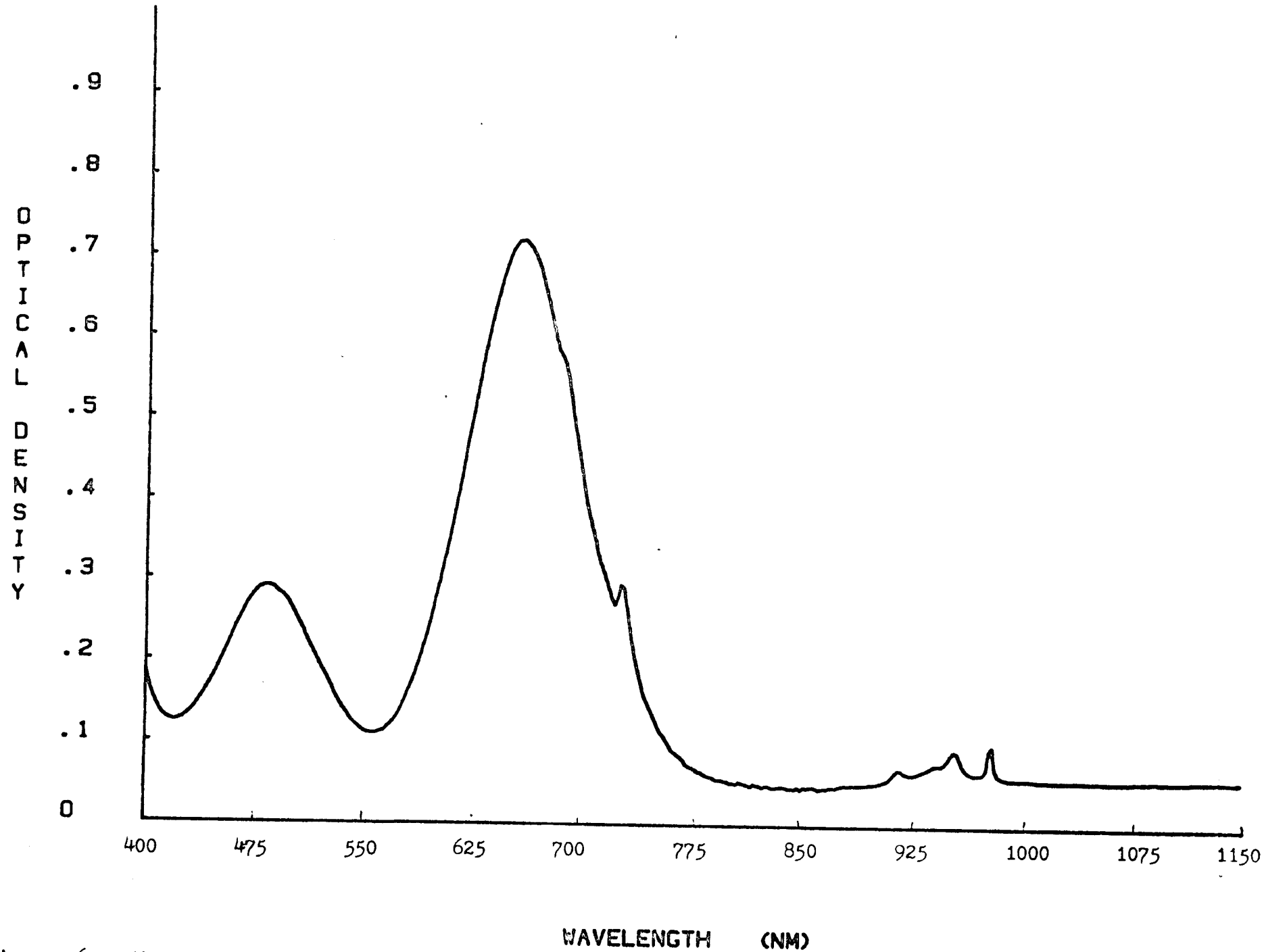

Figure 6. Absorption spectrum of Yb in $LiNbO_3$:Mg,Cr.

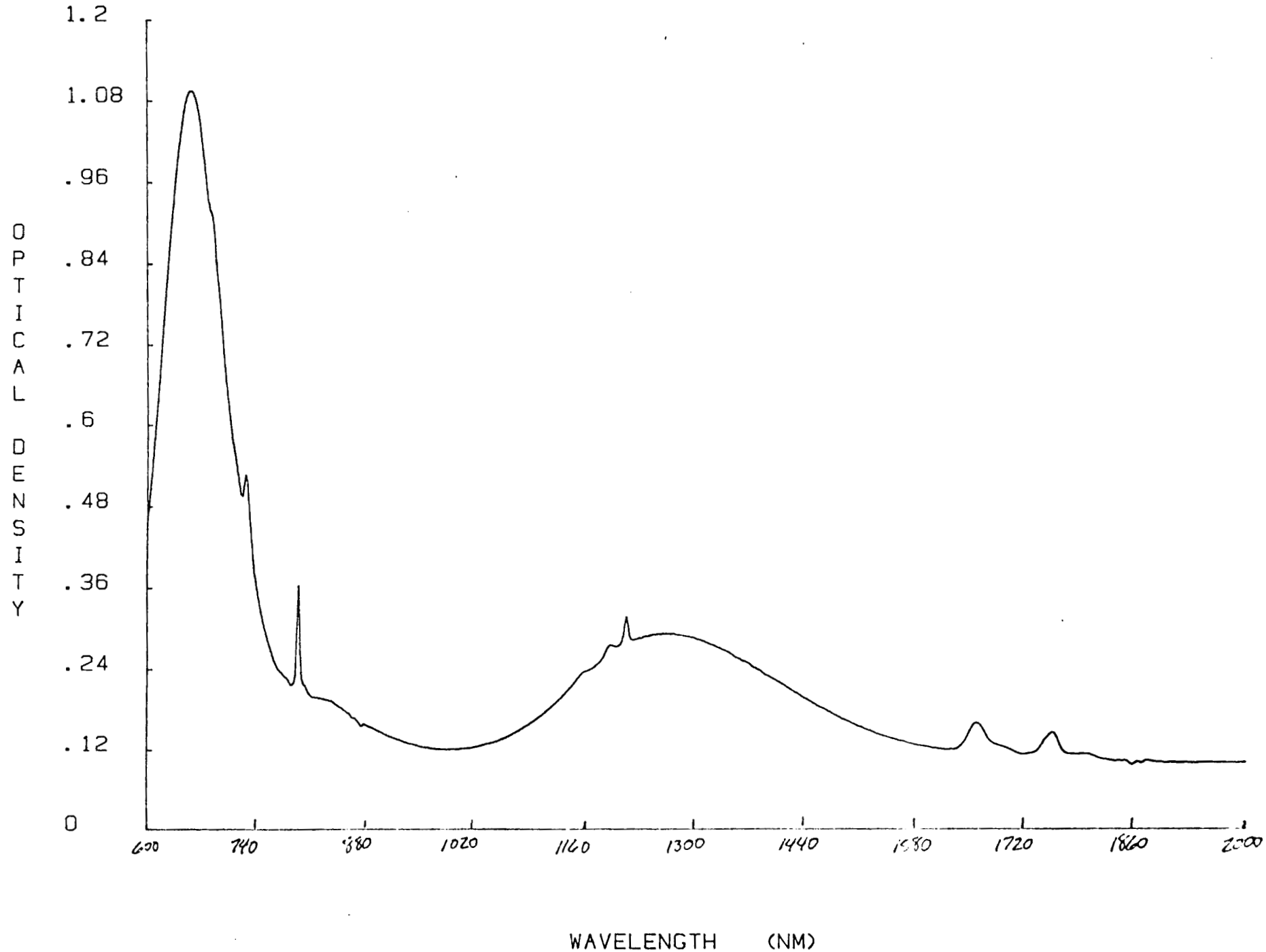

Figure 7. Absorption spectrum of Tm in $LiNbO_3$:Mg,Cr.

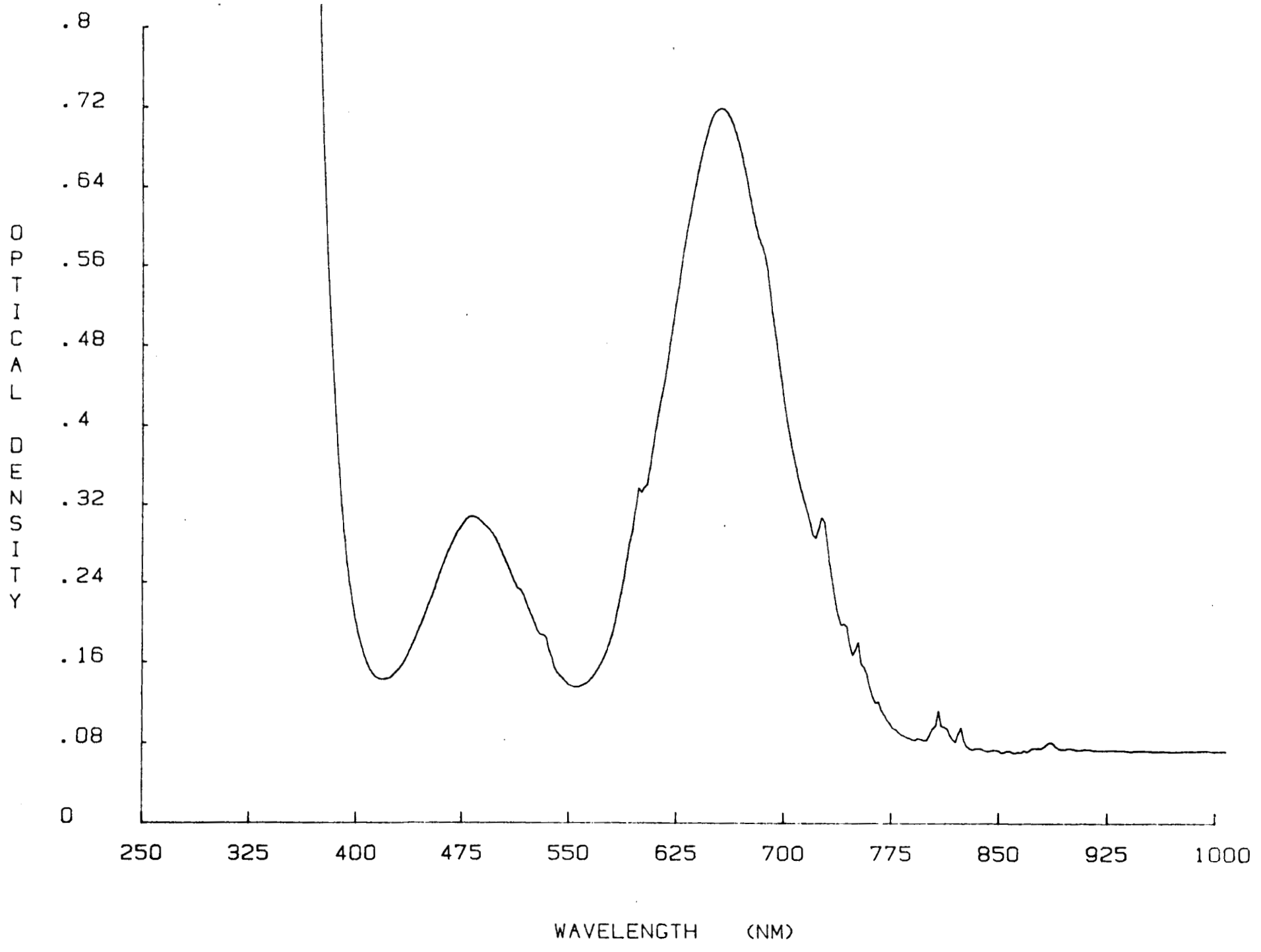

Figure 8. Absorption spectrum of Nd in $LiNbO_3$:Mg, Cr.

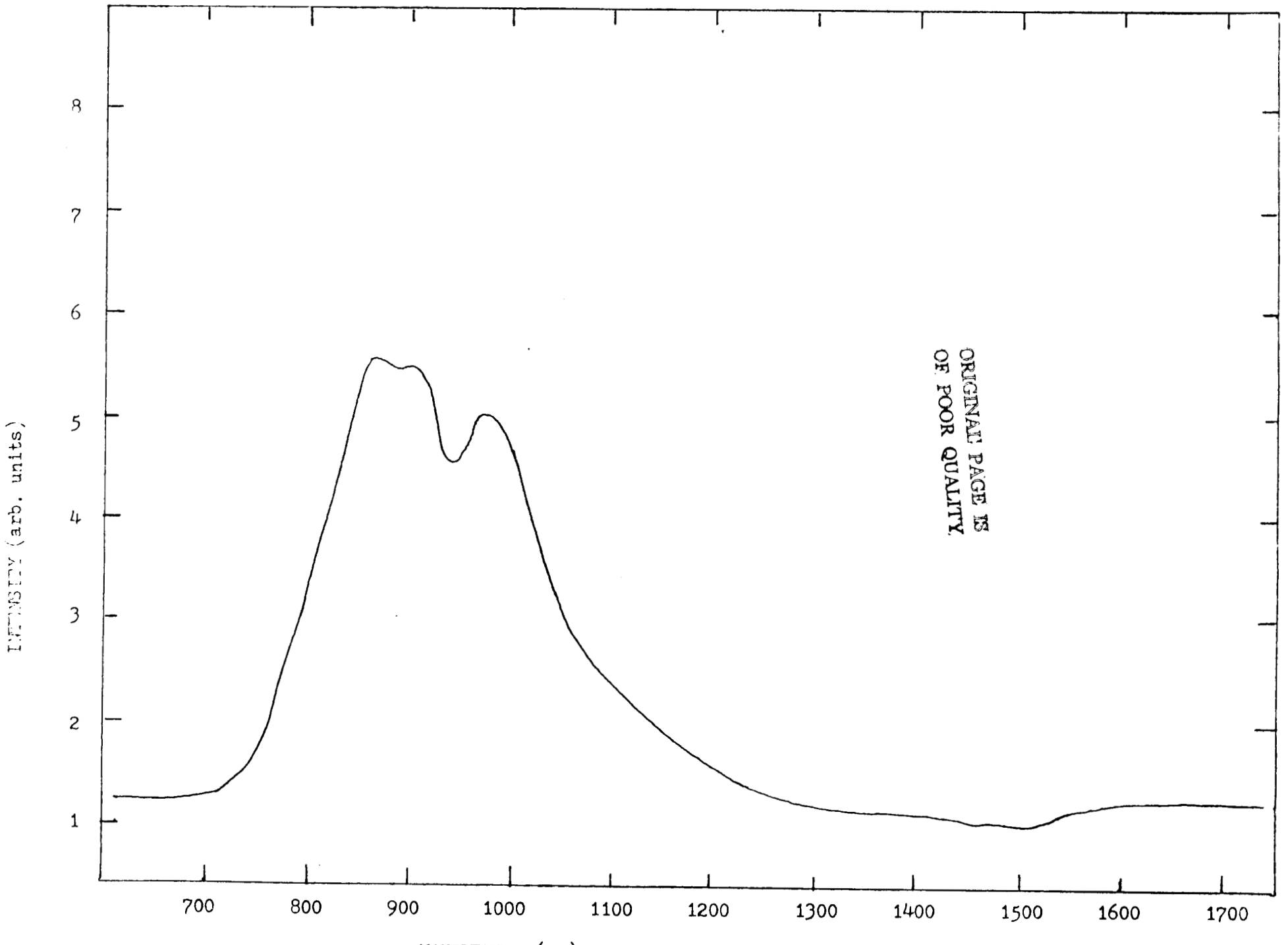

Figure 9. Fluorescence of $LiNbO_3$:Mg,Cr,Er pumping Cr.

Figure 10. Fluorescence of $LiNbO_3$:Mg,Cr,Yb pumping Cr.

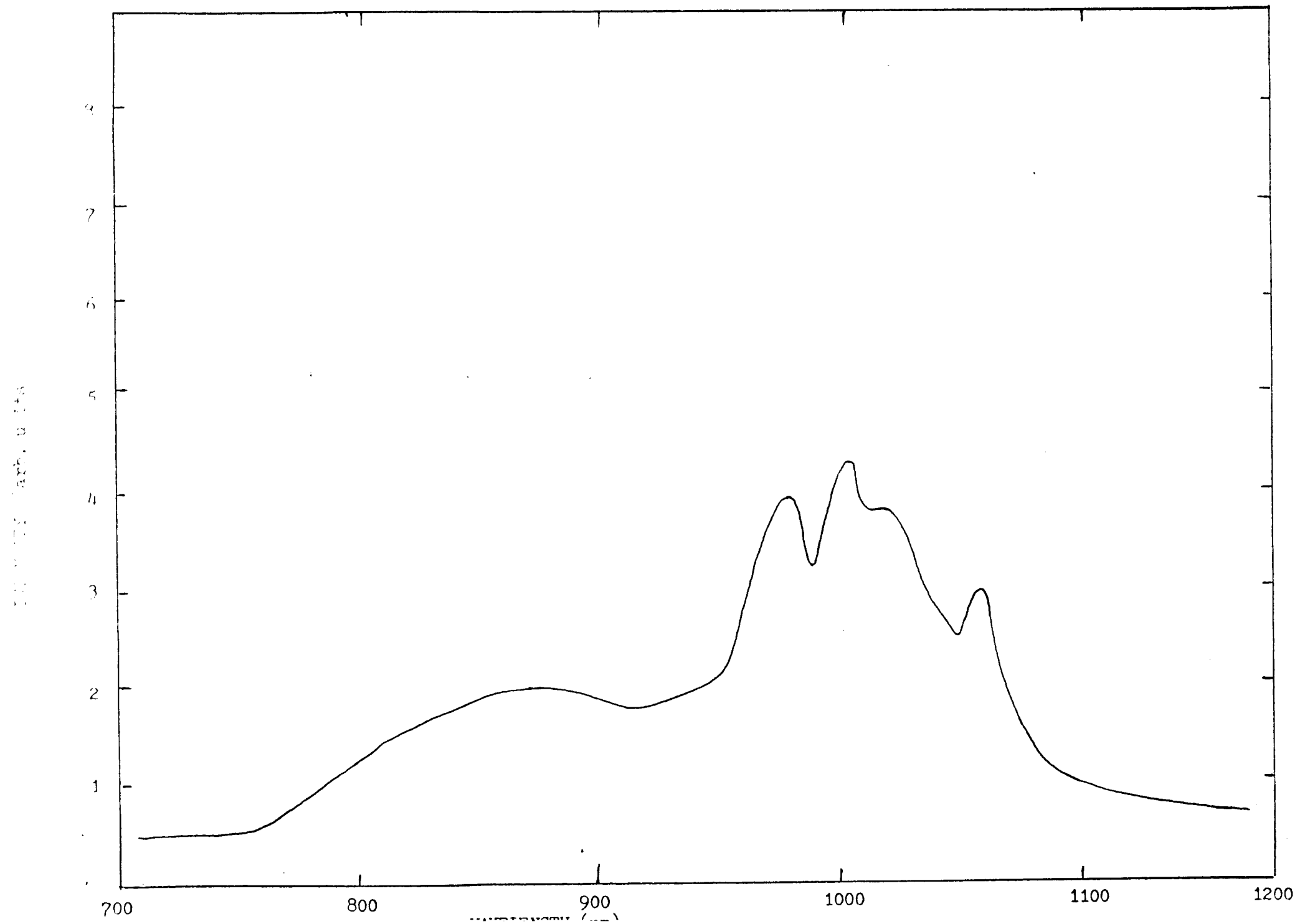

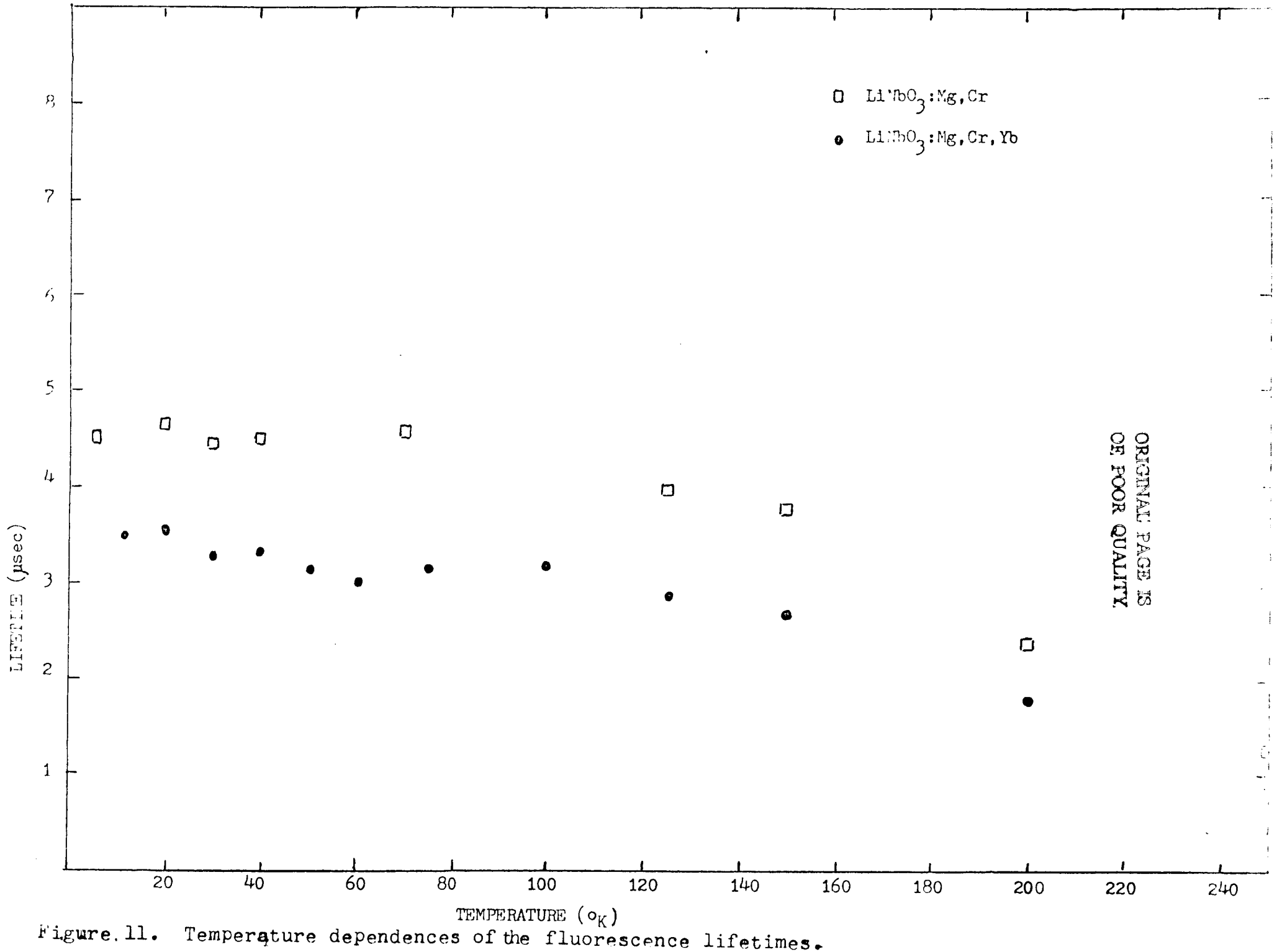

Figure.11. Temperature dependences of the fluorescence lifetimes.

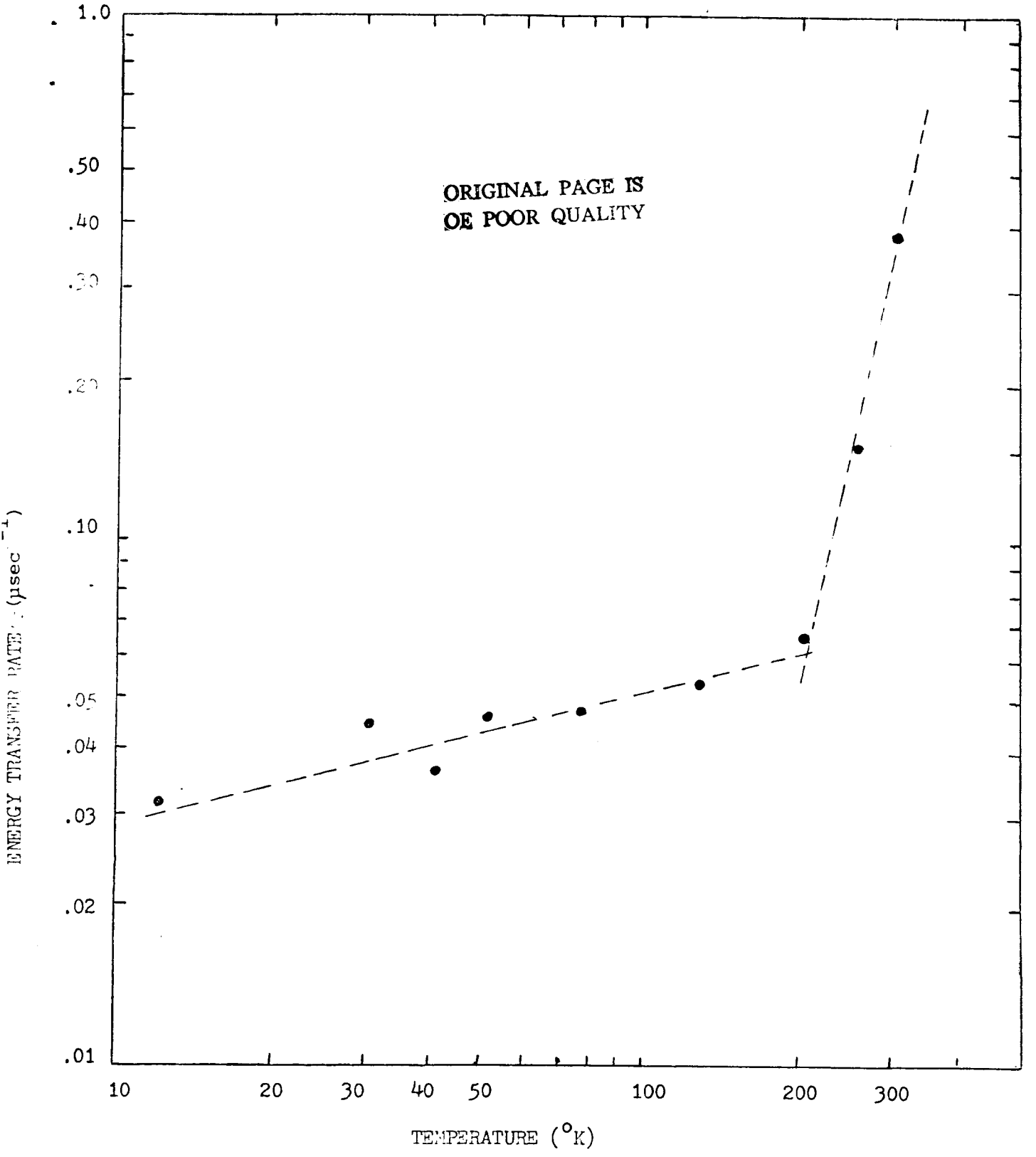

Figure 12. Temperature dependence of the Cr-Yb energy transfer rate.